JOURNAL OF GEOPHYSICAL RESEARCH, VOL. 113, C06024, doi:10.1029/2007JC004132, 2008

Variability of the Kuroshio Current south of Sagami Bay as observed using long-range coastal HF radars

Steven R. Ramp,[1] Donald E. Barrick,[2] Tomotaka Ito,[3] and Michael S. Cook[4]

Received 29 January 2007; revised 12 December 2007; accepted 30 January 2008; published 24 June 2008.

[1] Ocean surface currents between Cape Nojima and Hachijo Island have been mapped since fall 2000 using a pair of SeaSonde long-range HF radars. During September 2000 through December 2001, the no large meander (NLM) nearshore (n) and offshore (o) modes were observed. The surface current maps allowed new details to be observed in the structure of these modes and the transitions between them. Two noteworthy phenomena include blocking of the surface currents when the Kuroshio was in an extreme nearshore position behind the Zenisu Ridge and the ''Kyucho'' pattern when the current retroflexed from the NLMo position. In early 2004, a large meander (LM) developed and was well established in its historical position south of Honshu by August 2004. Subsequently, the LM continued propagating downstream, but stopped when it encountered the Izu Ridge. It then moved back to its original position near 137.5°E, and the process repeated itself. This east-west oscillation resulted in two common positions for the LM south of Sagami Bay: from its more westerly position (LMw, for west) the Kuroshio had a very favorable approach to the deep gap between Miyake Island and the Zenisu Ridge, and the currents were strongly toward the northeast through the region. When the meander moved up against the ridge (LMe, for east), a strong along-ridge current toward the northwest was evident, which turned sharply northeast when it encountered the shallow Zenisu Ridge. The dominant timescale for this within-mode variability was about 30 days.

Citation: Ramp, S. R., D. E. Barrick, T. Ito, and M. S. Cook (2008), Variability of the Kuroshio Current south of Sagami Bay as observed using long-range coastal HF radars, *J. Geophys. Res.*, *113*, C06024, doi:10.1029/2007JC004132.

1. Introduction

[2] The Japan Coast Guard (JCG) has been operating two 5 MHz long-range SeaSonde HF radar systems continuously since August 2001 to remotely sense the ocean surface currents south of Japan. These radars are of the direction-finding type, consisting of one transmit and one receive antenna at each location [*Barrick et al.*, 1977]. One system is located on the mainland at Cape Nojima on the tip of the Boso Peninsula near the mouth of the Tokyo and Sagami Bays, and the second is on Hachijo Island 200 km to the south offshore atop the Izu Ridge (Figure 1). The Kuroshio Current often flows directly between the two radars at scales easily resolved by the 10-km range cells. The region experiences some of the heaviest ship traffic in the world, and an accurate knowledge of the surface currents is necessary for maritime safety, pollution control, and search and rescue operations. Additionally, the Kuroshio has the largest mass and heat transport of any current in the Northern Hemisphere and plays an essential role in the global heat balance and climate variability.

[3] The basic modes of Kuroshio path variability south of Japan are well known from previous work and include the large meander (LM) mode, the no large meander nearshore mode (NLMn), and the no large meander offshore mode (NLMo) [*Shoji*, 1972; *Kawabe*, 1985, 1995]. The large meander is unique to the Kuroshio and has been much studied both observationally and theoretically [*Masuda*, 1989; *Sekine*, 1990; *Endoh and Hibiya*, 2001]. It forms intermittently and lasts for periods ranging from many months to years. The transitions between the two NLM modes occur more frequently (months rather than years) [*Shoji*, 1972; *Kawabe*, 1986, 1989] and are relatively less well studied. During both the LM and NLMn modes the Kuroshio passes inshore (north) of Hachijo directly through the radar field of view thus providing the opportunity to construct detailed maps of the space/time variability of the near surface currents. The Kuroshio in the NLMo mode sometimes loops offshore south of Hachijo, but parts of it remain visible in the HF radar vector field.

[4] Recently, an east/west vacillation of the large meander was studied using a sigma coordinate, primitive equation numerical ocean model [*Mitsudera et al.*, 2006]. They attributed this vacillation of the LM to the baroclinic interaction of the deep flow beneath the Kuroshio with

[1] Monterey Bay Aquarium Research Institute, Moss Landing, California, USA.
[2] CODAR Ocean Sensors Ltd., Mountain View, California, USA.
[3] Hydrographic and Oceanographic Department, Japan Coast Guard, Tokyo, Japan.
[4] Department of Oceanography, Naval Postgraduate School, Monterey, California, USA.

0148-0227/08/2007JC004132$09.00

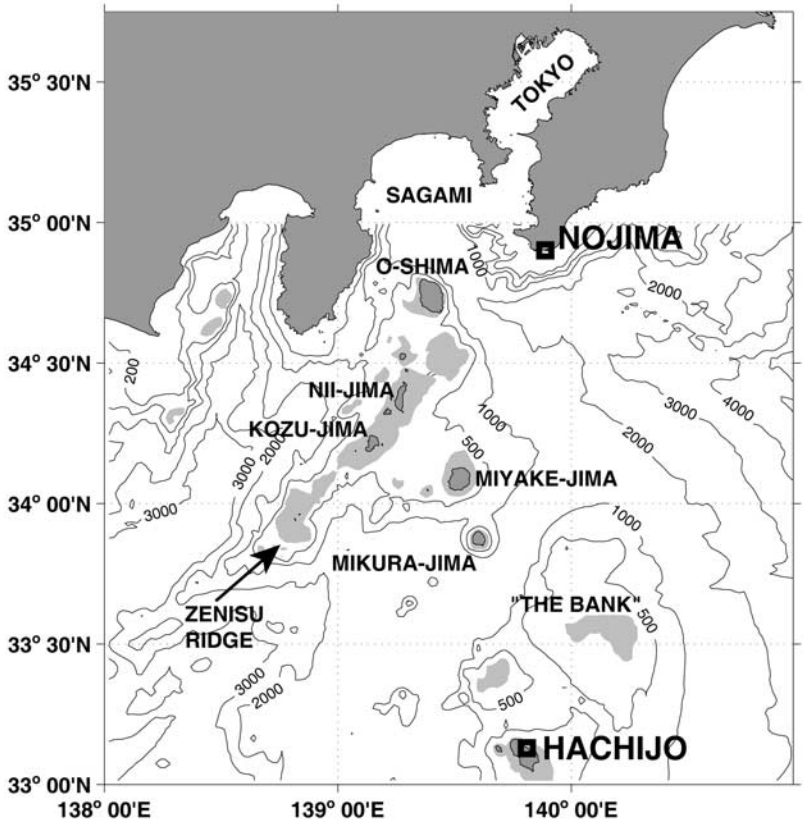

Figure 1. Base map for the geographic area covered by the Japan Coast Guard's long-range SeaSondes showing the site locations at Nojima and Hachijo, and important topographic features in between. The Izu Ridge runs straight south along the volcanic island chain delineated by O-shima, Miyake-jima, Mikura-jima, and Hachijo-jima. The Zenisu Ridge is a spur of the main ridge which runs southwest including Nii-jima and Kozu-jima. The gray shade indicates water less than 200 m deep. Other depth contours are as annotated.

the Izu Ridge (Joint Effects of Baroclinicity and Relief or JEBAR). The downslope flow in the deep water generated a cyclonic torque beneath the current which turned the current back away from the ridge. A term-by-term analysis indicated that this process was strong enough to overcome the barotropic tendency to generate anticyclonic vorticity by vortex compression as the current climbed the ridge. *Mitsudera et al.* [2006] lacked modern observations to compare the model results with, and this comparison will be taken up in the discussion section.

[5] In this paper, the surface currents south of Sagami Bay during the LM and NLM modes and the transitions between them are studied using the JCG HF radar data from August 2001 through December 2004. During 2001–2002, no large meander was present, and the work confirms the earlier results based on the coastal and island sea level data that there are at least two modes of variability present during the NLM time. New results show significant variation of the flow when the current was in the NLMn mode, depending on whether it was inshore or offshore of the Zenisu Ridge. Extreme positions during the NLMo phase also lead to Kuroshio retroflexions (westward flow) sometimes directly into Sagami bay. Beginning in July 2004 and continuing to the end of the year, the Kuroshio Current was in the large meander mode. We find that the current assumes two common positions during the LM mode, one located to the west (LMw) with the crest near 137.5°E, extending south to almost 30°N; and the second to the east (LMe) when the downstream side of the LM moved up against the Izu Ridge. In the remainder of this paper, these phenomena are described observationally in greater detail, and some comparisons with recent theory regarding the dynamics of the large meander are made.

2. Data and Methods

[6] The fundamental principle of surface current sensing via shore-based HF radar is that energy transmitted over the sea surface is Bragg-scattered back to the receiving antenna from the ocean surface wave whose wavelength is exactly half the wavelength of the transmitted signal. The frequency of the received signal is Doppler-shifted by an amount determined by the speed at which the Bragg wave is moving toward or away from the receive antenna. The speed of the wave itself is well known theoretically and is subtracted from the solution to reveal the speed of the underlying ocean surface currents. The distance to the backscattered signal is determined by range-gating the returns, and the angle it is coming from is determined by a direction-finding process [*Barrick and Lipa*, 1997] using three colocated receive antennas; two orthogonal closed loops and a single

monopole. The result from a single site is an omni-directional radial current map V(r, θ) emanating along "spokes" from the antenna location. If multiple sites are employed, the total vector maps **V**(x, y) may also be determined for the region of overlapping coverage via a straightforward geometry problem. This system very closely approximates a true surface current measurement: For the 5 MHz radars discussed here, the wavelength λ = 60 m and the effective depth of penetration into the ocean d = $\lambda/8\pi$ = 2.4 m [*Stewart and Joy*, 1974; *Paduan and Graber*, 1997].

[7] There are two types of errors that can reduce the accuracy of current maps from HF radars, namely systematic biases and statistical fluctuations. The latter have zero mean and originate from three sources: (1) The fact that the radar echo from Bragg-scattering ocean waves is a Gaussian random variable, representing a linear relationship to the Gaussian wave height itself. (2) Additive external noise originating from atmospheric and cosmic sources. (3) Subgrid-scale fluctuation of currents within the radar cell. All of these are zero mean, and are reduced by averaging at various levels in the signal processing. Systematic error stems primarily from imperfect knowledge of echo return location (bearing angle). This results from the receive antenna interacting with both natural and man-made objects around it which distorts the antenna pattern, causing echoes to be placed in the wrong location. This error is dealt with by calibrating the antenna patterns after installation using a transponder in a small boat whose position is always known [*Emery et al.*, 2004; *Ullman and Codiga*, 2004; *Paduan et al.*, 2006]. Using calibrated antenna patterns always improves HF radar accuracy, although the amount of improvement depends on the individual site, with some benefiting from the procedure more than others.

[8] To quantify the above errors in the real ocean, there have now been many studies comparing HF radar surface currents with other observations such as surface drifters, ship-mounted ADCPs, and moored ADCPs [*Emery et al.*, 2004; *Ullman and Codiga*, 2004; *Ebuchi et al.*, 2006; *Paduan et al.*, 2006]. These comparisons are always difficult since none of these instruments measure quite the same thing, and much of the "error" can be ascribed to natural variability in the environment [*Kohut et al.*, 2006]. The collective result from all of these studies is that HF radar error in surface current speed is most commonly about 7 cm s^{-1}, with the best result being 2.5 cm s^{-1} off New Jersey [*Kohut et al.*, 2006] and the worst 17–19 cm s^{-1} in the Soya Strait [*Ebuchi et al.*, 2006]. Since these errors are all well below the mean speed of the Kuroshio (100–150 cm s^{-1}) we conclude that the HF radar observations will have no difficulty discerning the path of the current in the observed surface current fields.

[9] The basic JCG data set consists of the radial current maps **V**(r, θ) from each site averaged and recorded every three hours. These maps are employed within the region of overlapping field of view to produce the total vector maps **V**(x, y), also at 3-hourly intervals. Ideal antenna patterns were used up through April 2004 and measured patterns were used after that. The measured patterns were very good, closely tracking the ideal patterns indicating that both antennas were well-sited and installed by the JCG. The two radars easily span the 200 km distance between them during the daytime, but the radar coverage was much reduced at night (the 9 P.M. and 12 midnight local time maps) owing to increased radio frequency noise in the area. To further improve the signal-to-noise ratio and reduce aliasing due to the tides, eight 3-h maps were averaged together to produce daily averaged representations of the surface currents between the two radars. Since the data are gridded and gap-free, the maps thus obtained also allow estimation of derivative quantities such as the divergence ($\nabla \cdot \mathbf{V}$) and curl ($\nabla \times \mathbf{V}$) of the flow, which provide some insight into the kinematics and dynamics of the transitions between current positions. Before gradient quantities were computed, the time series at each point were further smoothed using a low-pass filter with a half-power point of 33 h [*Beardsley et al.*, 1985]. This filter effectively removes the tidal and inertial energy, which is centered near 21 h at this latitude. Since the timescale for the mesoscale motions is typically two weeks or longer, the Nyquist Theorem is easily satisfied by the daily time series.

[10] When two HF radars are deployed horizontally opposed, current vectors along a line connecting the two radars (called the baseline) and a short distance to either side of the baseline are unresolved since radial velocity toward one site is the same as radial velocity away from the other. To fill in this region, an algorithm was developed at CODAR Ocean Sensors Ltd. which uses the observed along-radial component and a linearly interpolated cross-radial component using the first good data from either side of the baseline. While the distance to good data is variable in each map, the interpolated region was on average a diamond-shaped pattern about ±17 degrees to either side of the baseline.

[11] Sea level data around Japan are collected routinely in real time by the Japan Coast Guard and the Japan Meteorological Agency (JMA), and are available online at the Japan Oceanographic Data Center (JODC). The hourly data were daily averaged to reduce the tidal signal and were demeaned to produce the sea level anomalies used here. While more precise leveling information is available for each station, no attempt at absolute leveling was made as only the height fluctuations were of interest. Thus one cannot say at any time that one island station was higher or lower than the other. High versus low sea level as used in this paper are relative terms applicable to each individual station.

[12] Starting in 2003, a new product became available on line known as the Next Generation Sea Surface Temperature (NGSST) for the Open Ocean [*Lei and Kawamura*, 2004]. This technique objectively merges satellite sea surface temperature (SST) observations from Advanced Very High Resolution Radiometers (AVHRR), the Moderate Resolution Imaging Spectroradiometer (MODIS), and the Advanced Microwave Scanning Radiometer-EOS (AMSR-E) to produce quality-controlled, cloud-free, high spatial resolution (0.05 degree-gridded), daily SST maps. The details of how this is done as well as the digital data for each image can be found on the Web at http://www.ocean.caos.tohoku.ac.jp/~merge/sstbinary/actvalbm.cgi?eng=1. Microwave radiometers have the advantage of seeing through clouds, but have relatively poor spatial resolution. The infrared systems, when available, have excellent spatial resolution (order 1 km) but data are often missing owing to cloud cover. By objectively merging the two, NGSST produces daily maps preserving some of the mutual goodness of both

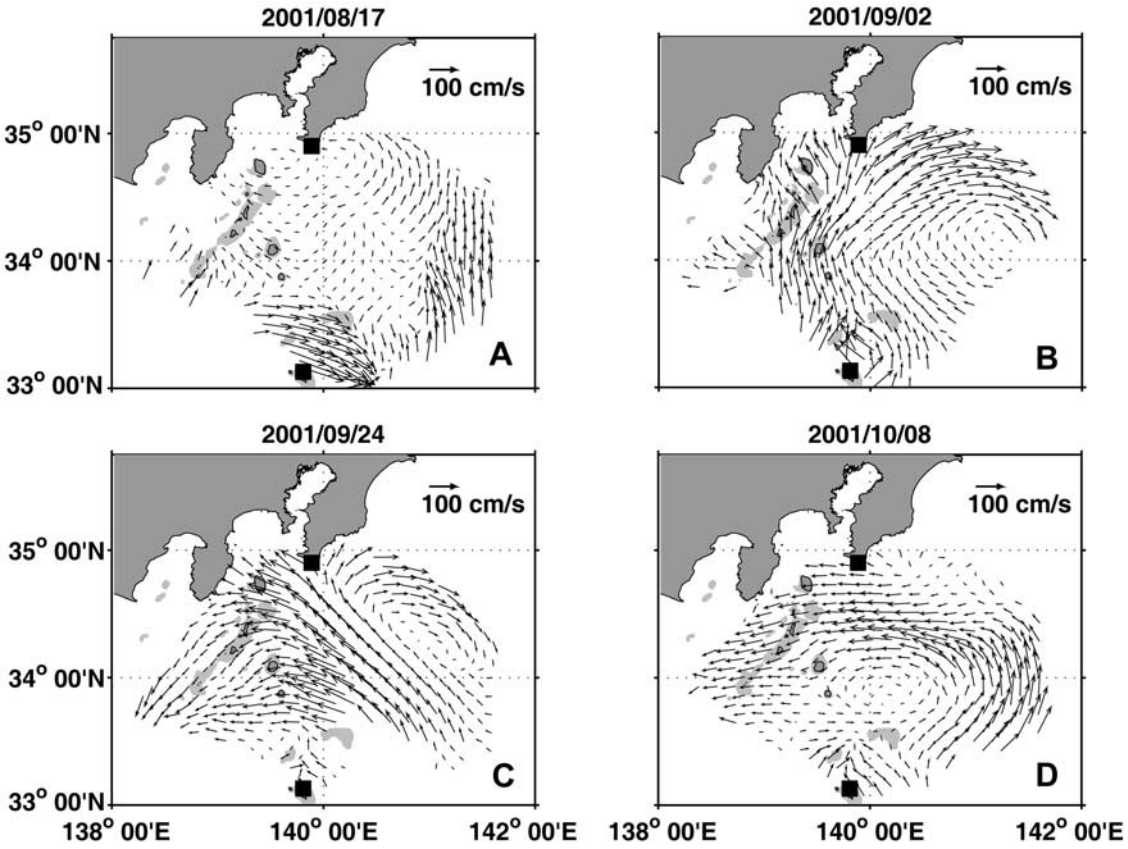

Figure 2. Maps showing typical surface current patterns for the Kuroshio no-large-meander offshore mode: (a) 17 August 2001; (b) 2 September 2001; (c) 24 September 2001; and (d) 8 October 2001. The current strength (cm/s) is indicated by the length of the arrow, according to the vector scale in the upper right corner of each plot.

systems. Since it is cloudy much of the time off southern Japan, the images are often heavily interpolated and smaller-scale features must be viewed with some caution. Larger-scale features however, such as the path of the Kuroshio, are fairly robust and the data availability (daily time series) is dramatically improved from earlier techniques. It is useful to overlay the HF radar surface current vectors on the NGSST images when available, and this has been done for the discussion of the LM mode during 2004.

3. Results

[13] The daily averaged currents show some remarkable flow patterns, most of which reflect the profound influence of the bottom topography on the path of the Kuroshio south of Japan (Figure 1). The Izu Ridge extends straight south, punctuated by a series of islands and shallow banks that breach (or near) the surface. Features to note include the unnamed shallow bank less than 139 m deep (hereafter "the bank") just north of Hachijo Island; the only channel deeper than 1000 m between the bank and Mikura Island; a second deep channel between Miyake Island and the Zenisu Ridge; and the Zenisu Ridge itself extending southwest from O-shima. The Zenisu Ridge is shallower than 200 m (shaded in gray) everywhere north of 33° 50′ N, 138° 30′ E and plays an important role in controlling the flow. Also important is the much deeper entrance to Sagami Bay via the eastern versus the western channel around O-shima.

[14] All the vector maps (Figures 2–5) show current maxima in the Kuroshio exceeding 1.2 m s^{-1} (2.4 knots) in agreement with previous investigators [*Taft*, 1972]. The pronounced along-stream variations observed have also been noted [*Taft*, 1972] but were poorly resolved by earlier observations. The slower surface currents in this region versus further upstream to the west (>2.0 m s^{-1}) likely result from bottom friction over the Izu Ridge impeding the Kuroshio which exceeds 1000 m depth elsewhere south of Japan [*Taft*, 1972; *Worthington and Kawai*, 1972; *Endoh and Hibiya*, 2001].

3.1. Surface Current Patterns

[15] Beginning with the NLM offshore mode, the Kuroshio path favored the channel between Hachijo Island and the bank, but the flow direction in the channel reversed according to the position of the downstream-propagating meanders. On 17 August (Figure 2a), a tight meander flowed through the southern corner of the radar field of view, with southeastward flow through the channel. By 2 September (Figure 2b), the meander in Figure 2a had propagated downstream out of the field of view and a second meander was approaching, forcing onshore (northwestward) flow from offshore of Hachijo. In this position, the flow passed northwestward through the channel then closely followed the Zenisu Ridge between Kozu Island and Miyake Island before splitting at Cape Nojima. This splitting of the current at Cape Nojima was observed frequently

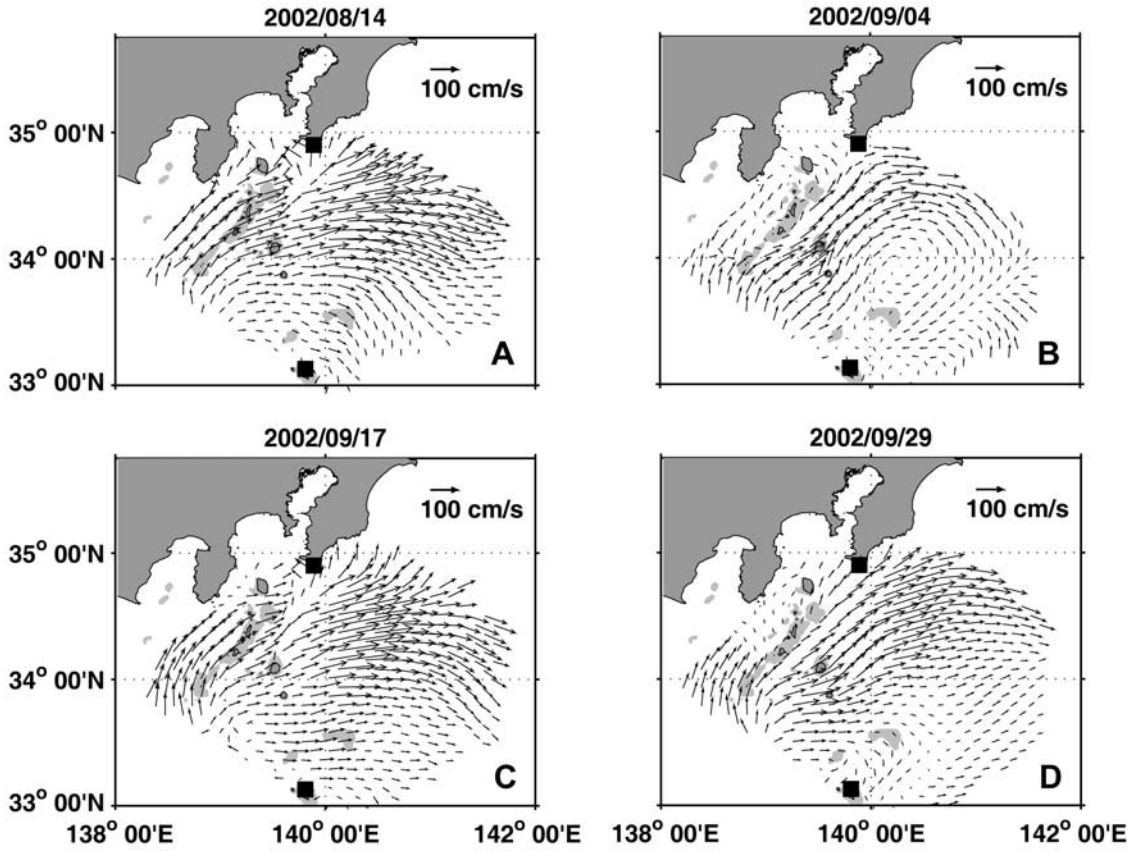

Figure 3. Maps showing typical surface current patterns for the Kuroshio no-large-meander nearshore mode: (a) 14 August 2002; (b) 4 September 2002; (c) 17 September 2002; and (d) 29 September 2002. The current strength (cm/s) is indicated by the length of the arrow, according to the vector scale in the upper right corner of each plot.

during the NLMo mode and during transitions between the LMw and LMe positions, discussed later. Most of the current then continued northeastward along the Japanese coast while a smaller fraction of the flow turned into Sagami Bay. Stronger flow into the bay was observed in late September and early October during a Kuroshio retroflexion. On 24 September (Figure 2c), the flow was directly into Sagami Bay via the deep eastern channel, almost unimpeded by topography. This flow mode may represent an explanation for the "Kyucho" ("swift currents") phenomenon when very fast, warm, high-salinity currents bring tuna into the bay and wreak havoc with drift net fishing [*Miura*, 1927; *Kimura*, 1942; *Uda*, 1953; *Matsuyama and Iwata*, 1977; *Yamagata*, 1980]. An even stronger retroflexion occurred on 8 October (Figure 2d) when the flow south of Nojima was actually westward.

[16] Four examples of important flow patterns observed during the NLM nearshore mode are shown in Figure 3. Especially noteworthy was the blocking of the Kuroshio by the Zenisu Ridge when the current approached the ridge from the west in an extreme nearshore position (Figures 3a and 3c). On 14 August 2002 (Figure 3a) the main current assumed this position behind the Zenisu Ridge and was blocked by topography creating a region of very weak flow in the lee of the ridge. By 4 September (Figure 3b), the current had migrated offshore of the ridge and flowed through the region unimpeded. A second example of the position shift is shown for 17–29 September (Figures 3c and 3d). This flow pattern was repeated many other times during the observation period and is believed to be robust. This fluctuating flow path was also evident in the island sea level data (Figure 6, top). Sea level was high at both Miyake and Hachijo on 14 August and 17 September, indicating a Kuroshio position inshore of both islands. Subsequently, sea level was high at Hachijo but low at Miyake on 4 and 29 September, indicating a position further offshore between the two islands. Historical hydrographic data show that the deeper currents at 400 m flow around the ridge even when the Kuroshio is close to the shore [*Kawabe*, 1985, 1986].

Figure 4. Maps showing surface current patterns overlaid on the NGSST satellite sea surface temperature images during the Kuroshio large meander mode. The sequence from top to bottom represents one transition from the LMw to the LMe position. The inset shows the larger-scale Kuroshio position as indicated by the JCG "quick bulletin of ocean conditions" plots for the same day. The data are from: (a) 20 September 2004, LMw; (b) 24 September 2004, transitioning; and (c) 2 October 2004, LMe. The SST scale is shown as a color bar to the right, with the blue shades being cooler and red warmer.

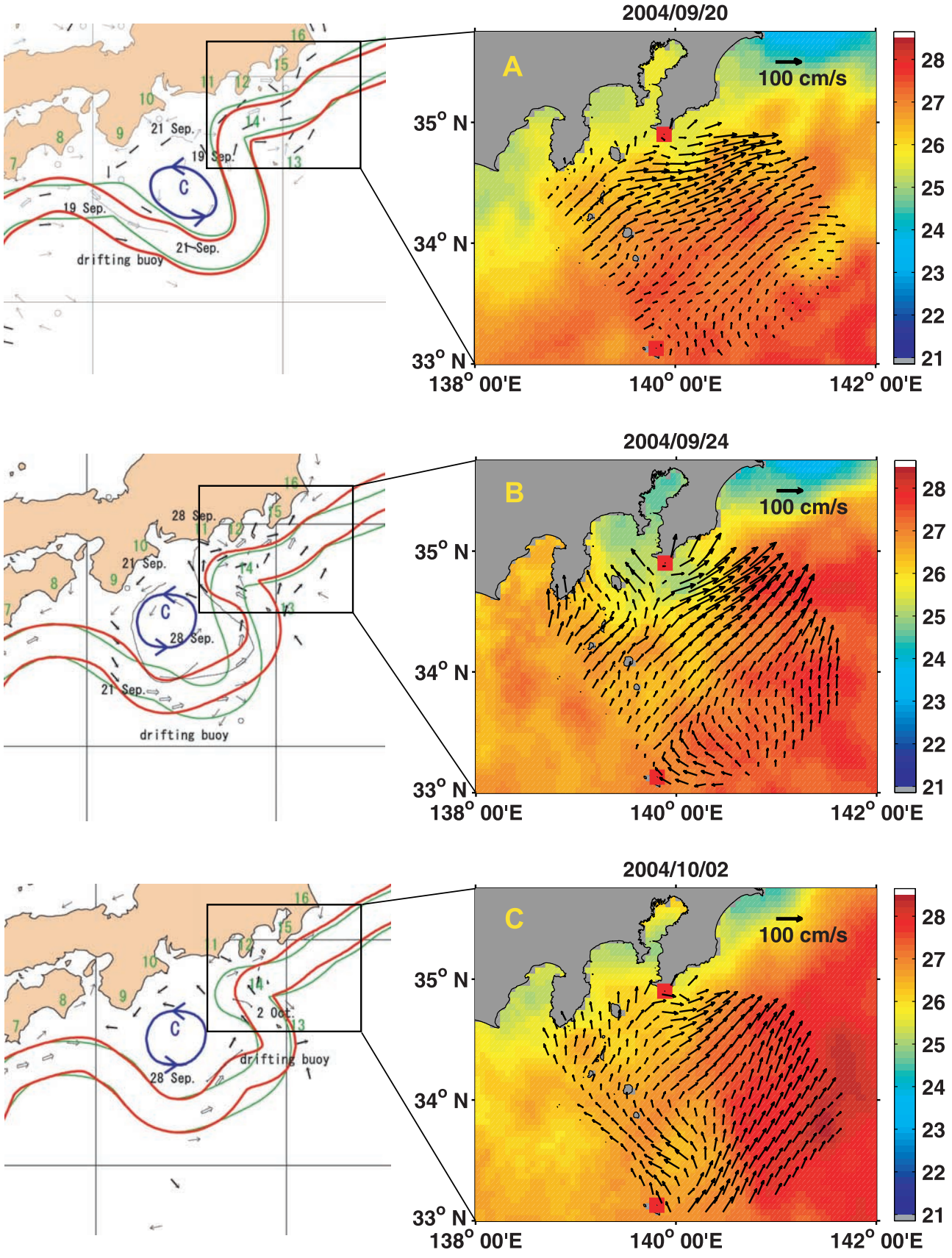
2004/09/20
A
100 cm/s
35° N
34° N
33° N
138° 00'E
140° 00'E
142° 00'E
21 Sep.
19 Sep.
C
19 Sep.
21 Sep.
drifting buoy
2004/09/24
B
100 cm/s
28 Sep.
21 Sep.
C
28 Sep.
21 Sep.
drifting buoy
2004/10/02
C
100 cm/s
2 Oct.
C
28 Sep.
drifting buoy

Figure 4

We hypothesize that the deep flow spins up the near-surface currents again downstream of the ridge.

[17] Two three-map sequences of surface current vectors from late 2004 overlaid on the NGSST sea surface temperature product show the progression from the LMw to the LMe position (Figures 4 and 5). In the LMw position, the current had the best possible approach to the deep gap in the Izu Ridge just north of Miyake Island. The result was very strong currents to the northeast, virtually unobstructed by topography (Figure 4a). This corresponds to the ''typical'' LM path as described by *Kawabe* [1985]. As the current transitioned from the LMw to the LMe position, it took a more northeastward approach to the deep gap in the Izu Ridge and looked similar to some NLMo realizations with pronounced splitting of the current at Cape Nojima (Figure 4b). This can also be seen in the NGSST image as cooler water at the Cape. The 2 October map shows one of the most extreme LMe positions observed, both in the current maps (Figure 4c) and sea level (Figure 6, bottom). In this position the current flowed northwest parallel to the western flank of the Izu Ridge, then turned sharply northeast as it approached the Zenisu Ridge. This represents the usual case in most of the LMe maps. In this extreme case, the current split at Hachijo Island with some of the current flowing northeast and some flowing northwest. However, the Kuroshio subsequently retreated back to the LMw position once again, as evidenced by both sea level and subsequent surface current maps (Figure 5).

[18] A similar sequence during November 2004 (note the slightly cooler sea surface temperatures) also shows the transition from the LMw to the LMe position (Figure 5). The current pattern in the top panel closely resembles Figure 4a, with the Kuroshio west of the Izu Ridge, turning slightly along the offshore side of the Zenisu Ridge. On November 28 (Figure 5b) the current position was similar to Figure 4b with the corresponding splitting and cooler water at Cape Nojima. The bottom panel (Figure 5c) is a typical LMe picture, with most of the flow going northwest along the flank of the Izu Ridge, turning northeast at the Zenisu Ridge.

[19] These movements during the LM mode can also be tracked in the sea level data (Figure 6, bottom). From the LMw position, the current was inshore of both Hachijo and Miyake, and the sea level at both stations was high. During the LMe events, the surface current was adjacent to Hachijo Island and the sea level there was low, but remained high at Miyake. The extreme eastward event, from which the current subsequently retreated, is obvious in the figure as the large depression spanning 20 September to 4 October.

[20] The coastal and island sea level changes during the various current positions described above are summarized in Table 1. The LM versus NLM modes are easily distinguished by the sea level difference between the Kushimoto and Uragami stations, as described by previous authors [e.g., *Kawabe*, 1995]. For the NLMo mode, the current loops offshore south of both Hachijo and Miyake and both stations are low. During NLMn, the current is always inshore of Hachijo so this station is high, but Miyake may be high or low, depending on whether the current is in its nearshore or extreme nearshore (behind the Zenisu Ridge) position. When the Kuroshio was in its classical LM position [*Kawabe*, 1985, 1995], the main current passed inshore of both islands and sea level was high. However, we demonstrate here that the current repeatedly moved east and flowed parallel to the western flank of the Izu Ridge before retreating to its original position. During these eastward excursions, sea level dropped at Hachijo but remained high at Miyake.

3.2. Time Series and Autospectra

[21] Because these observations provide continuous time series of the surface currents at every grid point, the timescales of the variability can be quantified by plotting these time series and calculating the autospectra from selected key locations around the region. It has been shown in the Santa Barbara Channel that autospectra calculated from HF radar time series were identical to autospectra from ADCPs at the same point for periods longer than 10 h [*Emery et al.*, 2004]. Time series are shown (Figure 7, locator map Figure 8) for the channel between Miyake Island and the Zenisu Ridge (grid point 68), and for three points located to the east of the ridge nearshore (grid point 262), toward the middle of the vector field (grid point 275) and offshore (grid point 286). The dashed vertical line in early January demarks a rather obvious change in the currents when the Kuroshio switched from the NLMo to the NLMn mode. Before the switch, currents were weak in the channel (grid point 68) but strong offshore (grid point 286). The offshore time series showed strong periodicity during the NLMo mode as meanders passed by. During the NLMn mode (after the dashed line), the currents offshore were low, and the currents in the channel were high but fluctuating, depending on whether the current was inshore or offshore of the Zenisu Ridge. A clear inverse correlation can be seen between grid point 68 and Miyake sea level. During the high sea level events, the current was behind the Zenisu Ridge and the currents in the channel were weak. During the low sea level events, the Kuroshio was clear of the ridge and the currents in the channel were high. During May 2002, a meander passed through the region during the NLMn time which elevated the currents at the offshore point and weakened (near zero) the flow in the channel. This was a rare event that occurred only once between February 2002 and February 2003.

[22] The autospectra (Figure 8) can be used to statistically quantify the variability that is easily visible by eye in Figure 7. These autospectra were piece-averaged using sixteen 480 $\times$ 3 h pieces smoothed with a Hanning window and overlapped by 50%. This procedure results in 32 degrees of freedom and resolves periods out to 60 days. Three different timescales emerge from the autospectra, with significant peaks at 30 d, 10 d, and 3–5 d. The 30-d peak was prominent in all the time series. During the NLMo mode, this was the period with which meanders propagated downstream past the mooring. During the NLMn mode, this was the period of the current wandering to either side of the Zenisu Ridge. Away from the Izu Ridge (grid points 262 and 275) a 10-d peak appeared which had more energy than the 30-d peak. This may represent higher-frequency meandering in the region to the east of the ridge where the flow is not constrained by bottom topography. The 3–5 days peaks, which are usually ascribed to the local synoptic-scale weather patterns, were present at all locations. These peaks might also represent along-axis variability of the along-

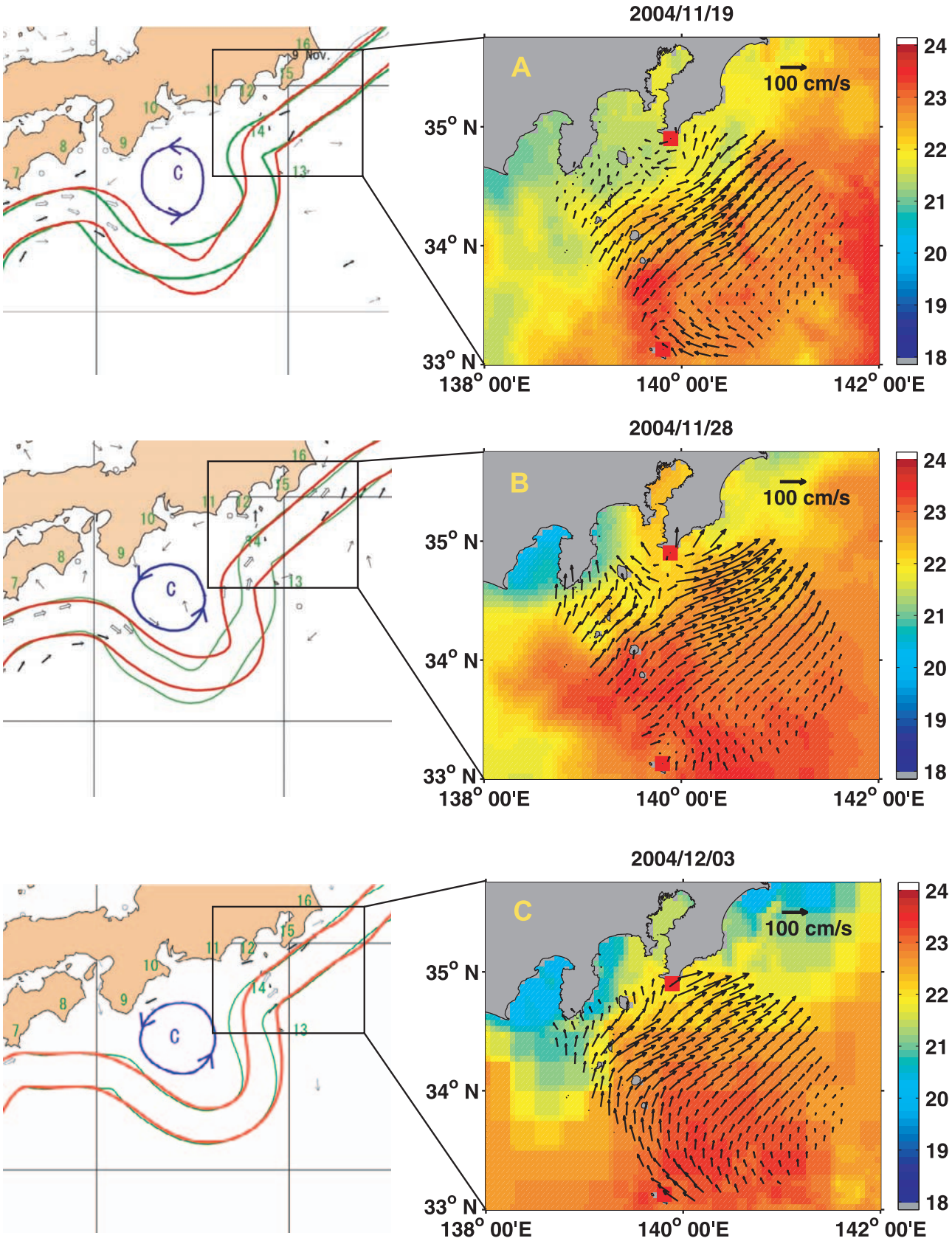

Figure 5. As in Figure 4 except for a second sequence from (a) 19 November 2004, LMw; (b) 28 November 2004, transitioning; and (c) 3 December 2004, LMe.

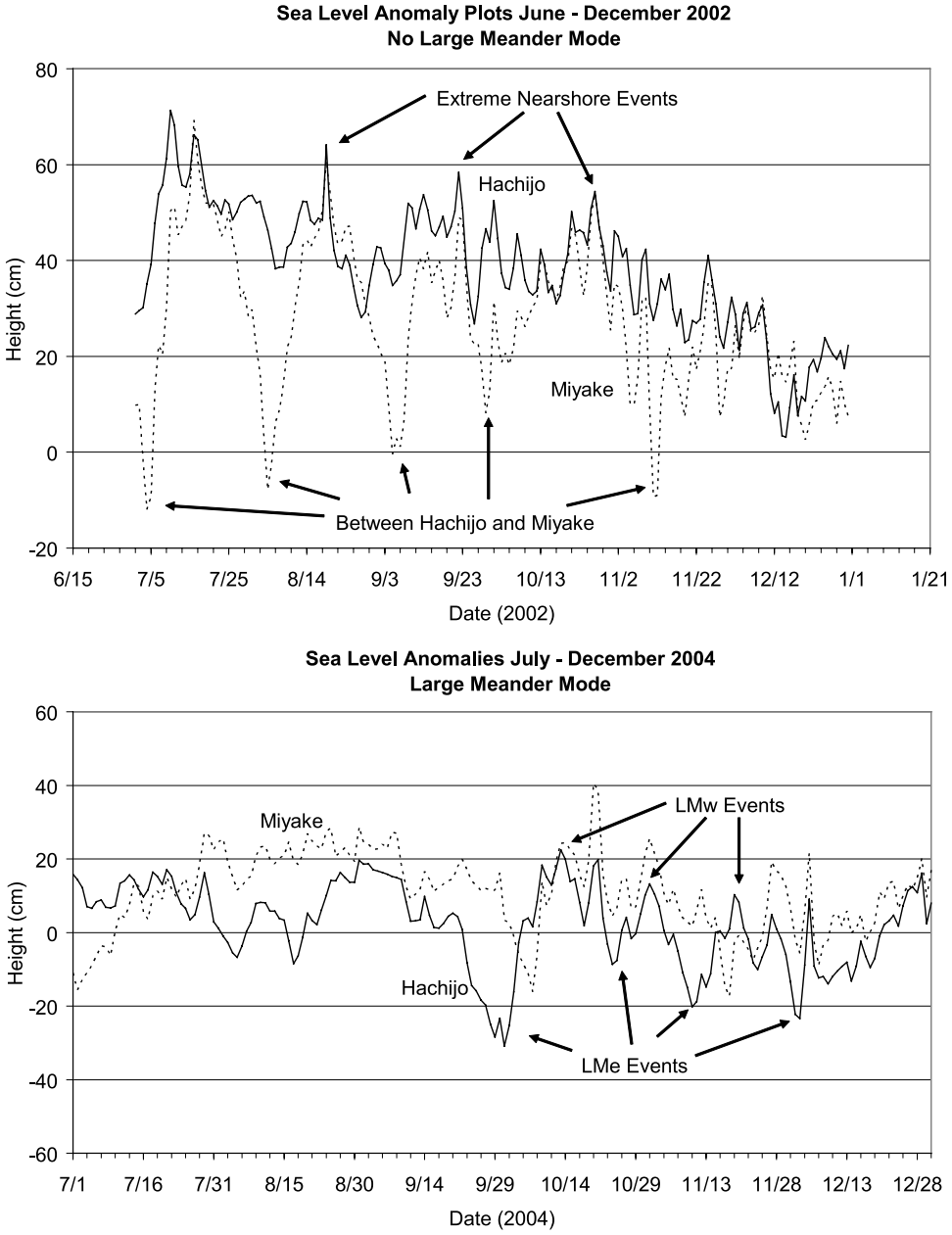

Figure 6. Island sea level anomalies for (top) the NLM modes and (bottom) the LM modes during 2002 and 2004, respectively. In both plots, sea level at Miyake Island is shown by a dotted line and at Hachijo Island by a solid line.

current flow, which is visually evident in movies assembled from the surface current maps. The dynamics of these motions are unknown, but merit further investigation. The total energy of the flow was greatest at the nearshore (262) and middle (275) locations, which were downstream from the deepest channels and therefore the least impeded by bottom friction.

[23] Time series plots of the north-south (v) component from January 2004 to April 2005 (Figure 9) show how the currents changed as the large meander was established during late July 2004. The currents in the deep channel between Miyake Island and the Zenisu Ridge (point 1) became strong and remained strong throughout the LM mode, since most of the Kuroshio passed through this channel regardless of whether the current was in the LMw or LMe position. This was also true at point 4, which was located downstream from the channel. The LMw/LMe oscillation was most evident at points 2 and 3 where the current was weak in the LMw mode but strongly northward during the LMe mode (Figure 9). This was because the main

Table 1. A Summary of the Coastal and Island Sea Level Heights During the Current Positions Observed Using the HF Radar Data

Location	NLMn Blocked	NLMn Unblocked	NLMo	LMw	LMe
Miyake	high	low	low	high	high
Hachijo	high	high	low	high	low

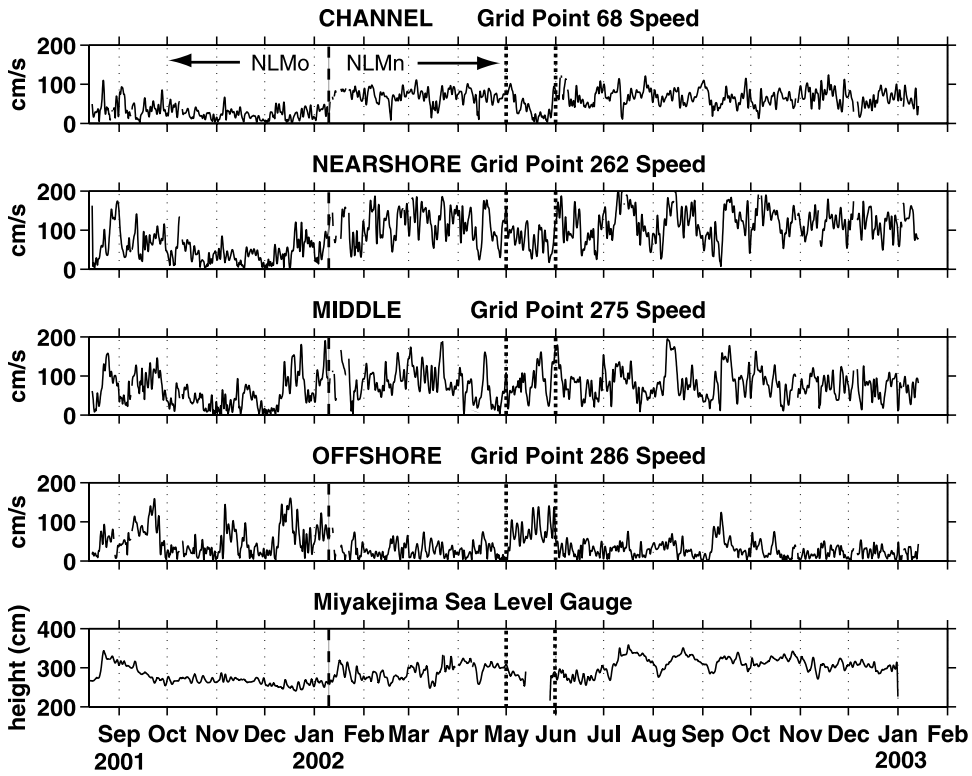

Figure 7. Time series plots of the current speed (vector sum of u and v) for selected grid points within the HF radar coverage, whose locations are shown in the top left plot of Figure 8. The bottom plot indicates sea level at Miyake Island for comparison. The vertical dashed line indicates the change from the NLMo to the NLMn mode. The vertical dotted lines frame a meander which passed by later during the NLMn mode, most evident by the inverse correlation between the channel and offshore time series.

current was located to the north of these points in the LMw mode but directly over them in the LMe mode. This allows a convenient way to quantify the period of the LMw/LMe oscillation. The peak-to-peak elapsed times for the LMe mode at observation point 2 were 45, 32, and 60 days respectively for the events indicated on the Figure. Statistically, the autospectrum from point 2 (not shown) showed that the period of the oscillation was centered on 30 days.

[24] Also noteworthy in Figure 9 is the exceptionally strong LMe event during October 2004, when the current split around Hachijo (Figure 4c). This event was observed as a northward pulse at location 5, where the other LMe events were not observed. Finally, strong anticyclonic eddies sometimes form on the offshore side of the Kuroshio. An example from March 26, 2004, shown in Figure 9 (top plot), shows one such eddy that reversed the currents at points 5 and 6, as indicated in Figure 9 (bottom two plots).

4. Analysis and Discussion

4.1. Impacts on Primary Production

[25] Ocean surface color images often reveal very high spatial variability in the chlorophyll *a* concentrations within the region covered by the JCG HF radars. By superimposing the surface current vector maps (or derived quantities such as the divergence and curl) on the satellite-sensed ocean color fields, the underlying processes associated with some of the high pigment concentration regions is revealed. We intuitively expect at least two basic mechanisms leading to high chlorophyll *a* concentrations: (1) Persistent surface current divergence and upwelling leads to high local in situ production and growth, and (2) material may be concentrated in convergent zones by horizontal advection of high chlorophyll *a* waters from elsewhere. Examples of both mechanisms have been observed in the region south of Sagami Bay.

[26] On 26 May the Kuroshio turned sharply northward just after crossing the Izu Ridge and flowed straight toward Cape Nojima (Figure 10a). The current then split offshore from the cape with most of the current continuing northeastward and a smaller fraction heading northwest toward Sagami Bay. As described earlier, this was a fairly common flow pattern that was observed during both the NLMo and LM modes. The current split at Nojima created a region of high divergence (5×10^{-5} s^{-1}) near the cape (Figure 10b) which was also associated with very high plant pigment concentrations. The divergence is slightly higher but the same order of magnitude as the divergence due to wind-driven upwelling north of Point Reyes ($2-3 \times 10^{-5}$ s^{-1}) also calculated from HF radar data filtered and averaged in a similar way [*Kaplan and Largier*, 2006]. The high biological activity likely resulted from nutrients upwelling in the divergent zone accompanied by relatively slow horizontal advection which allowed the organisms there to flourish. The vertical velocity in the upwelling center can be estimated by integrating the horizontal divergence over an assumed mixed layer depth (MLD). Using the maximum

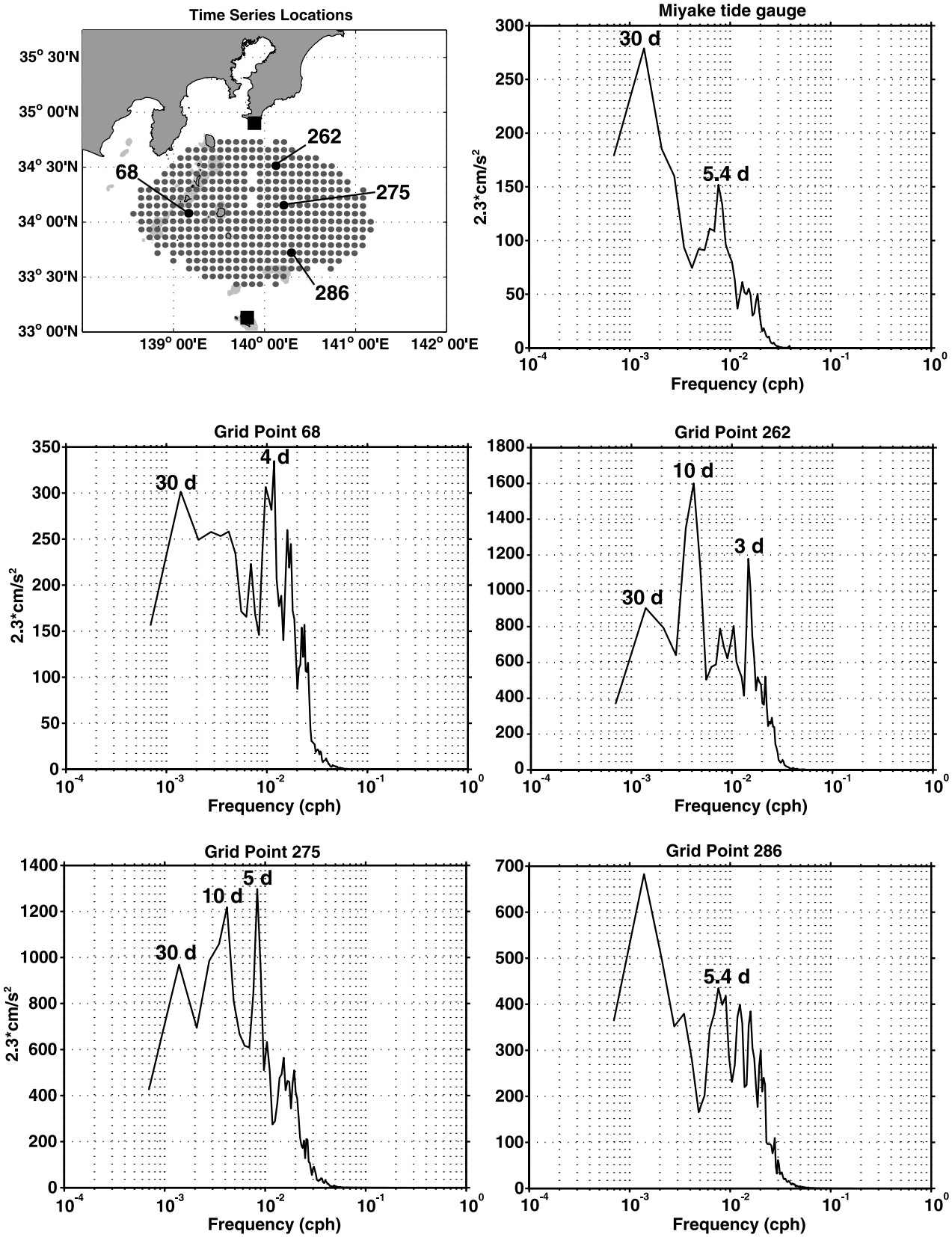

Figure 8. Variance-conserving autospectra for the time series shown in Figure 7. The period (hours) of the major peaks has been annotated for clarity. The physical meaning of the energy peaks is described in the text.

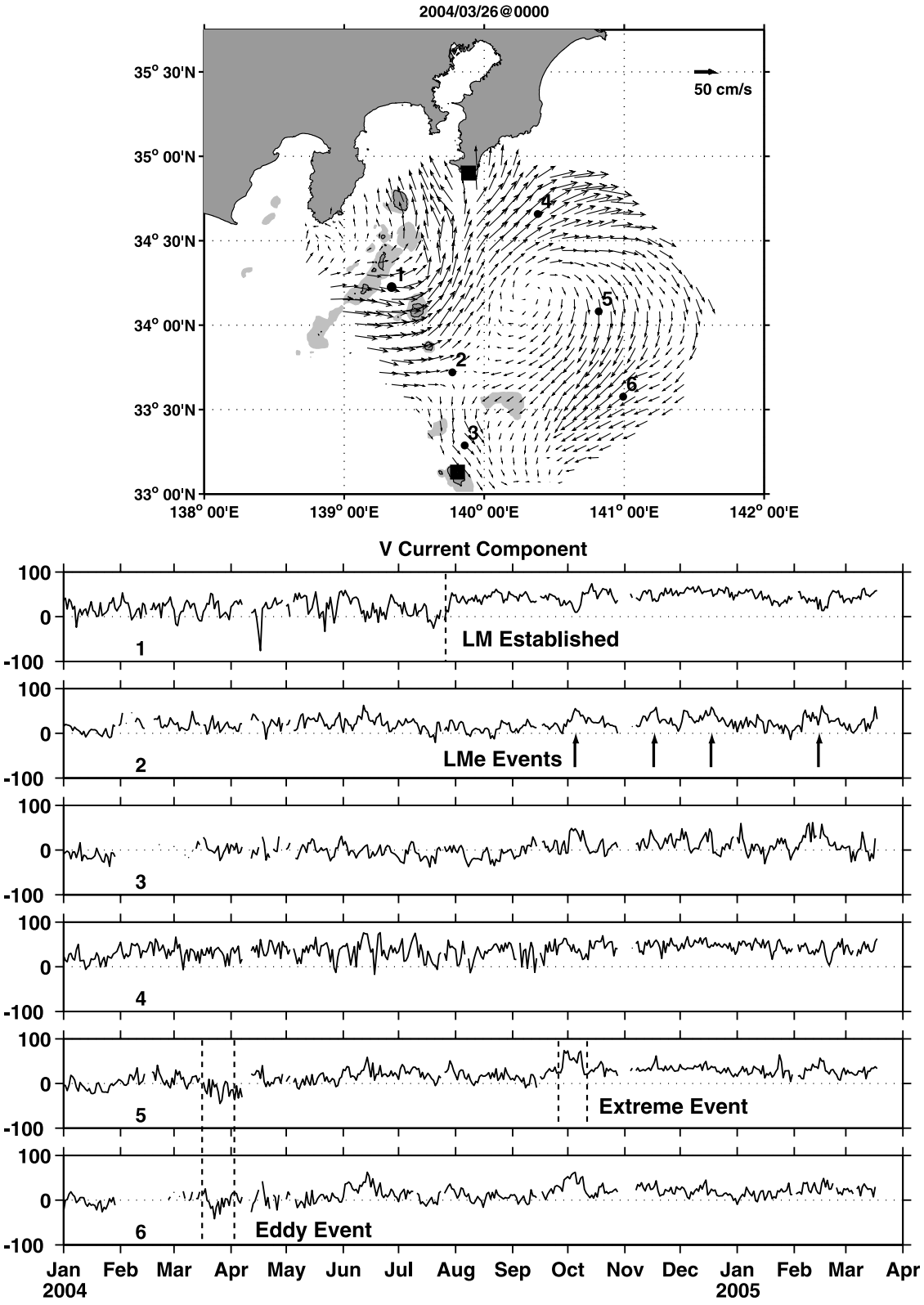

Figure 9. (top) Station locations for the time series shown in the bottom panel, overlaid on the surface current vector plot from 26 May 2004. Station locations for grid points 1, 4, 5, and 6 are similar to, but not exactly the same as the station locations used in Figures 7 and 8. (bottom) Selected time series of the north-south (v) current component from January 2004 to April 2005. Some key events are labeled and described in the text.

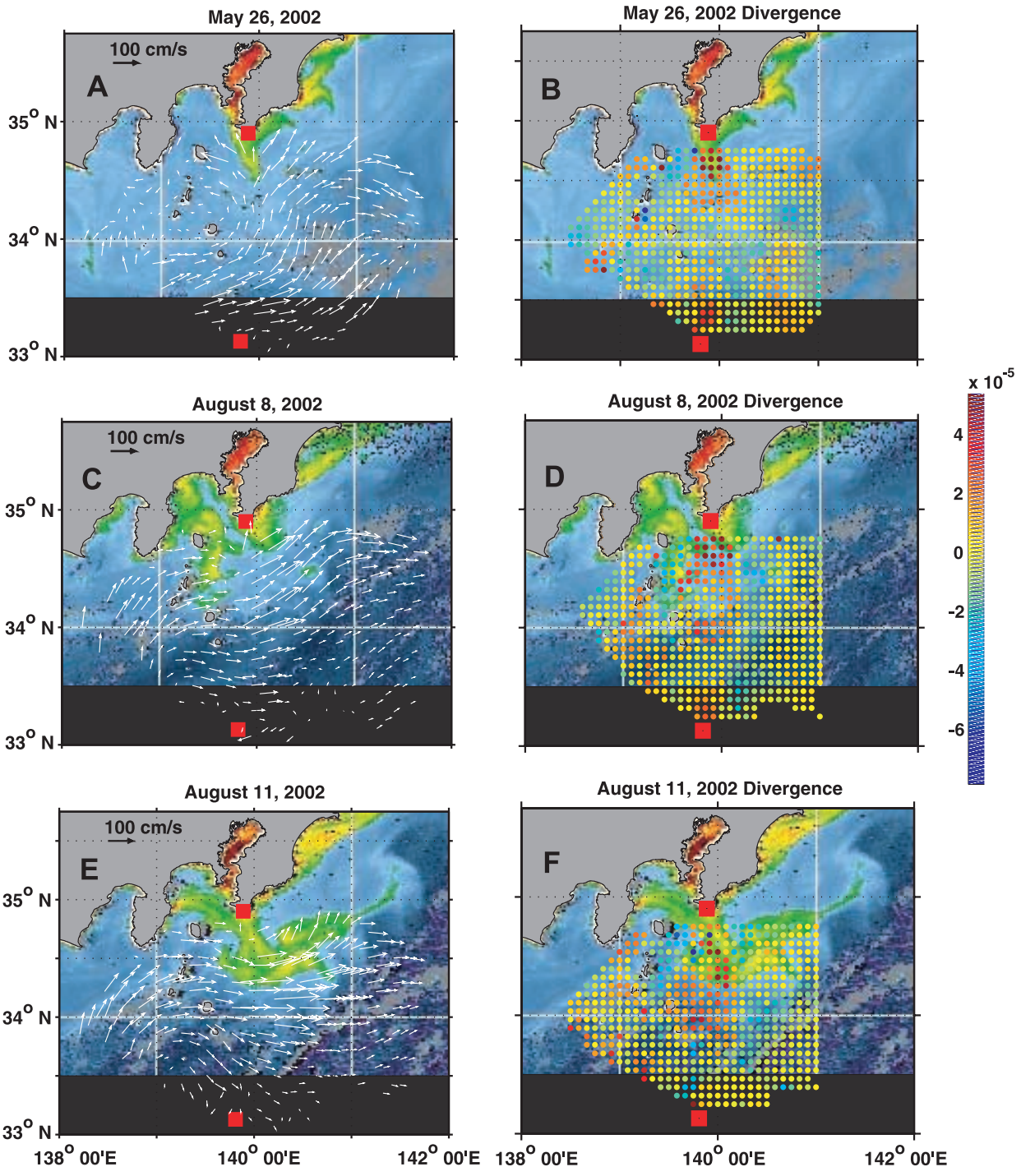

Figure 10. (a, c, e) Surface current vector fields and (b, d, f) dot plots of the low-pass filtered horizontal divergence superimposed on the surface chlorophyll *a* distribution computed from the SeaWiFS ocean color sensor. The color bar at right center indicates the scale of the divergence, with positive (red) indicating divergent flow and negative (blue) indicating convergent flow. The images are from (top) 26 May, (middle) 8 August, and (bottom) 11 August 2002.

observed divergence of 5×10^{-5} s^{-1} and an estimated spring MLD of 25 m gives a vertical velocity of order 100 m d^{-1}. This is considerably larger than typical values for wind-driven coastal upwelling which are only about 20 m d^{-1} for strong events [*Rudnick and Davis*, 1988]. The number is not inconceivable however for a totally different mechanism, or perhaps indicates a much shallower mixed layer at the time the observations were made which would reduce the estimated value. Error in the divergence estimate itself also contributes: Even after strong smoothing both temporally and spatially, the error in the divergence calculation from gridded HF radar data

is likely about the same as the magnitude of the divergence itself [*Kaplan and Lekien*, 2007]. The divergence patterns in the JCG HF radar data are nevertheless consistent from day to day and in visual agreement with the low-pass filtered current vector patterns.

[27] By contrast, two regions of high pigments offshore were observed on 8 August 2002 (Figure 10c). During this time, both the current vectors and SST show that the Kuroshio was in an extreme onshore NLMn position similar to the one shown in Figures 3a and 3c. A region of high surface pigment concentrations appeared once again associated with the current divergence near Cape Nojima, but there was also a second region of high pigments in the lee of the Zenisu Ridge in a region of high (about -3×10^{-5} s^{-1}) horizontal convergence (Figure 10d). These high pigment values apparently originated within Sagami Bay and were concentrated in this area by the highly convergent flow. Thus, two very different mechanisms were at work to produce the chlorophyll *a* patterns observed on 8 August. The material in the lee of the ridge was subsequently swept downstream when the Kuroshio moved back offshore on August 11, 2002 (Figures 10e and 10f). These overlays collectively illustrate how small changes in the Kuroshio path are extremely important in determining the distribution of near-surface chlorophyll *a* in the region south of Sagami Bay.

4.2. Some Dynamical Comments

[28] Many papers have been written on the origin, growth, and downstream propagation of the large meander. The consensus opinion is that the LM results from a combination of high-volume transport, baroclinic instability enhanced by the Koshu Seamount, and interaction with an offshore anticyclonic eddy [e.g., *Sekine*, 1990; *Endoh and Hibiya*, 2001; *Waseda et al.*, 2003]. Little has been written however about why the meander stops propagating downstream, although it was noted in some modeling results that the large meander did not form without the Izu Ridge [*Sekine*, 1990].

[29] Using the numerical model described in the introduction, it has been suggested that the LM not only stops, but rather vacillates between the east and west positions with a timescale of about 50–100 days [*Mitsudera et al.*, 2006]. For the example they show it took about 30 days for the LM to move from the western to eastern position, where the flow roughly paralleled the Izu Ridge. An interesting detail of the flow evolution was the northward movement of the axis of the Kuroshio along the western slope of the Izu Ridge. Comparison with some hydrographic surveys from the sixties and seventies showed general agreement with the model results.

[30] As summarized in Figure 9, the observations presented here allow quantification of the timescales for these motions. Our estimate for a complete cycle LMe to LMw and back to LMe ranged from 32 to 60 days with an average of 44 days, in reasonable agreement but slightly shorter than the model results. The surface current maps (Figures 4c and 5c) show that the surface flow toward the northwest diverged from the ridge, i.e., was downslope over the western flank of the ridge, when the current was in its most extreme LMe position. While we have no estimate of the deep flow at this time, this suggests that there may also be a barotropic component to the flow separation problem, which would tend to accelerate the mechanism and shorten the timescales. Animations of the surface current maps do not show the northward propagation of the axis along the ridge. Again per Figure 9, the current always preferred the channel between Miyake Island and the Zenisu Ridge when in either LM position, and the flow was anchored there. When the LM moved eastward from its traditional position, it struck the ridge more or less broadside.

[31] *Mitsudera et al.* [2006] do not discuss the possible impact of the angle of incidence of the Kuroshio axis relative to the Izu Ridge axis on the downstream propagation problem. In the NLM mode, when only small meanders are present, the current makes a nearly normal approach to the ridge, finds one of the "gates", and continues downstream. In the LM mode however, the current approaches the ridge from a much more oblique angle, whence it attempts to follow f/H contours to the north. For future work, we suggest a theoretical or numerical study which examines the importance of the strike angle of the current on topography.

[32] We further suggest that once it is established, the LM will oscillate in this way until some external process such as another interaction with an offshore eddy breaks down this cycle. These eddies are thought to originate in the Kuroshio extension and propagate westward under the planetary β effect [e.g., *Waseda et al.*, 2003; *Mitsudera et al.*, 2006]. Since both the eddy formation and the path the eddies follow westward are nondeterministic processes, the lifetime of the LM will likewise be highly variable.

5. Conclusions

[33] Three years of surface current data collected by the Japan Coast Guard HF radars located at Cape Nojima and Hachijo Island have revealed previously unknown details of the Kuroshio Current flow structure in this region. The observations allow us to quantify the space and timescales of the flow variability and transition between states. The basic flow patterns observed are variants of the well known no large meander nearshore, no large meander offshore, and large meander modes. Within the NLMn mode, the along-axis current speed was a strong function of whether the main current was positioned inshore or offshore of the Zenisu Ridge. Offshore of the ridge, the current passed freely through the deep passage between Miyake Island and the Zenisu Ridge. Inshore of the ridge, the flow was blocked by the ridge leading to a region of slow flow in the lee of the ridge. Within the LM mode, the current oscillated between two positions, namely the classical position to the west and a position flowing northwest along the Izu Ridge to the east. Time series of current velocity at selected points within the HF radar grid allow quantification of the periods of variability. Both the inshore (NLMn) oscillation and the offshore LM oscillation had a spectral peak centered on 30 days.

[34] The observed flow patterns are consistent with satellite-sensed sea surface temperature and ocean color maps, and show that high chlorophyll *a* results from both divergence and upwelling near Cape Nojima and concentration of near-surface pigments by convergent flows behind the Zenisu Ridge. Future work includes studying the transition

from the LM to the NLM mode, which did not happen during this HF radar observation period, and more detailed dynamical studies of the flow over topography.

[35] **Acknowledgments.** The authors are indebted to the men and women of the Japan Coast Guard for maintaining the HF radar systems and providing these high-quality data sets. Bob Arnone (Naval Research Laboratory, Stennis Space Center) provided the SeaWiFS imagery used in Figure 10.

References

Barrick, D. E., and B. J. Lipa (1997), Evolution of bearing determination in HF current mapping radars, *Oceanography*, *10*, 72–75.

Barrick, D. E., M. W. Evans, and B. L. Weber (1977), Ocean surface currents mapped by radar, *Science*, *198*, 138–144, doi:10.1126/science.198.4313.138.

Beardsley, R. C., R. Limeburner, and L. K. Rosenfeld (1985), Introduction to the CODE-2 Moored Array and Large Scale Data Report, in CODE-2: Moored array and large scale data report, *WHOI Tech. Rep85–35*, 234 pp., Woods Hole Oceanogr. Inst., Woods Hole, Mass.

Ebuchi, N., Y. Fukamachi, K. I. Ohshima, K. Shirasawa, M. Ishikawa, T. Takatsuka, T. Daibo, and M. Wakatsuchi (2006), Observation of the Soya Warm Current using HF ocean radar, *J. Oceanogr.*, *62*, 47–62, doi:10.1007/s10872-006-0031-0.

Emery, B. M., L. Washburn, and J. A. Harlan (2004), Evaluating radial current measurements from CODAR high-frequency radars with moored current meters, *J. Atmos. Oceanic Technol.*, *21*, 1259–1271, doi:10.1175/1520-0426(2004)021<1259:ERCMFC>2.0.CO;2.

Endoh, T., and T. Hibiya (2001), Numerical simulation of the transient response of the Kuroshio leading to the large meander formation south of Japan, *J. Geophys. Res.*, *106*, 26,833–26,849, doi:10.1029/2000JC000776.

Kaplan, D. M., and J. Largier (2006), HF radar-derived origin and destination of surface waters off Bodega Bay, California, *Deep Sea Res., Part II*, *53*, 2906–2930, doi:10.1016/j.dsr2.2006.07.012.

Kaplan, D. M., and F. Lekien (2007), Spatial interpolation and filtering of surface current data based on open-boundary modal analysis, *J. Geophys. Res.*, *112*, C12007, doi:10.1029/2006JC003984.

Kawabe, M. (1985), Sea level variations at the Izu Islands and typical stable paths of the Kuroshio, *J. Oceanogr. Soc. Jpn.*, *41*, 307–326, doi:10.1007/BF02109238.

Kawabe, M. (1986), Transition processes between the three typical paths of the Kuroshio, *J. Oceanogr. Soc. Jpn.*, *42*, 174–191, doi:10.1007/BF02109352.

Kawabe, M. (1989), Sea level changes south of Japan associated with the non-large-meander path of the Kuroshio, *J. Oceanogr. Soc. Jpn.*, *45*, 181–189, doi:10.1007/BF02123462.

Kawabe, M. (1995), Variations of current path, velocity, and volume transport of the Kuroshio in relation with the large meander, *J. Phys. Oceanogr.*, *25*, 3103–3117, doi:10.1175/1520-0485(1995)025<3103:VOCPVA>2.0.CO;2.

Kimura, K. (1942), On "Dai Kyucho" along coast, (in Japanese), *Chuoo Kishoodai Iho*, *19*, 1–85.

Kohut, J. T., H. J. Roarty, and S. M. Glenn (2006), Characterizing observed environmental variability with HF Doppler radar surface current mappers and acoustic Doppler current profilers: Environmental variability in the coastal ocean, *IEEE J. Oceanic Eng.*, *31*, 876–884, doi:10.1109/JOE.2006.886095.

Lei, G., and H. Kawamura (2004), Merging satellite infrared and microwave SSTs: Methodology and evaluation of the new SST, *J. Oceanogr.*, *60*, 905–912.

Masuda, A. (1989), A laboratory experiment on the Kuroshio meander, *Deep Sea Res.*, *36*, 1067–1081, doi:10.1016/0198-0149(89)90078-2.

Matsuyama, M., and S. Iwata (1977), The Kyucho in Sagami Bay, (in Japanese), *Suisan Kaiyo Kenkyukaiho*, *30*, 1–7.

Mitsudera, H., B. Taguchi, T. Waseda, and Y. Yoshikawa (2006), Blocking of the Kuroshio large meander by baroclinic interaction with the Izu Ridge, *J. Phys. Oceanogr.*, *36*, 2042–2059, doi:10.1175/JPO2945.1.

Miura, S. (1927), Studies on destructions of drift nets, *Teichi Gyogyoo Kai*, *1*, 4–21.

Paduan, J. D., and H. C. Graber (1997), Introduction to high-frequency radar: Reality and myth, *Oceanography*, *10*, 36–39.

Paduan, J. D., K. C. Kim, M. S. Cook, and F. P. Chavez (2006), Calibration and validation of direction-finding high frequency radar ocean surface current observations, *IEEE J. Oceanic Eng.*, *31*, 862–875, doi:10.1109/JOE.2006.886195.

Rudnick, D. L., and R. E. Davis (1988), Mass and heat budgets on the Northern California Continental Shelf, *J. Geophys. Res.*, *93*, 14,013–14,024, doi:10.1029/JC093iC11p14013.

Sekine, Y. (1990), A numerical experiment on the path dynamics of the Kuroshio with reference to the formation of the large meander path south of Japan, *Deep Sea Res.*, *37*, 359–380, doi:10.1016/0198-0149(90)90014-M.

Shoji, D. (1972), Time variation of the Kuroshio south of Japan, in *Kuroshio: Its Physical Aspects*, edited by H. Stommel and K. Yoshida, pp. 217–234, Univ. of Wash. Press, Seattle.

Stewart, R. H., and J. W. Joy (1974), HF radar measurement of surface current, *Deep Sea Res.*, *21*, 1039–1049.

Taft, B. (1972), Characteristics of the flow of the Kuroshio, in *Kuroshio: Its Physical Aspects*, edited by H. Stommel and K. Yoshida, pp. 165–216, Univ. of Wash. Press, Seattle.

Uda, M. (1953), On the stormy current ("Kyûtyô") and its prediction in the Sagami Bay, *I, J. Oceanogr. Soc. Jpn.*, *9*, 15–22.

Ullman, D. S., and D. L. Codiga (2004), Seasonal variation of a coastal jet in the Long Island Sound outflow region based on HF radar and Doppler current observations, *J. Geophys. Res.*, *109*, C07S06, doi:10.1029/2002JC001660.

Waseda, T., H. Mitsudera, B. Taguchi, and Y. Yoshikawa (2003), On the eddy-Kuroshio interaction: Meander formation process, *J. Geophys. Res.*, *108*(C7), 3220, doi:10.1029/2002JC001583.

Worthington, L. V., and H. Kawai (1972), Comparison between deep sections across the Kuroshio and the Florida Current and the Gulf Stream, in *Kuroshio: Its Physical Aspects*, edited by H. Stommel and K. Yoshida, pp. 371–386, Univ. of Wash. Press, Seattle.

Yamagata, T. (1980), A theory for propagation of an oceanic warm front with application to Sagami Bay, *Tellus*, *32*, 73–76.

D. E. Barrick, CODAR Ocean Sensors Ltd., 1914 Plymouth Street, Mountain View, CA 94043, USA.

M. S. Cook, Department of Oceanography, Naval Postgraduate School, 833 Dyer Road, Monterey, CA 93943, USA.

T. Ito, Hydrographic and Oceanographic Department, Japan Coast Guard, 5-3-1 Tsukiji, Chuo-ku, Tokyo 104-0045, Japan.

S. R. Ramp, Monterey Bay Aquarium Research Institute, 7700 Sandholdt Road, Moss Landing, CA 95039, USA. (sramp@mbari.org)